Fracture in microsphere monolayers studied by experiment and computer simulation

A. T. Skjeltorp* & Paul Meakin†

* Institute for Energy Technology, N-2007 Kjeller, Norway
† Central Research and Development Department,
E I du Pont de Nemours and Company, Wilmington,
Delaware 19898, USA

The formation of irregular (often fractal[1]) patterns under non-equilibrium conditions has become a subject of considerable scientific and practical interest. One of the most important processes of this type is the formation of cracks and other extended defects in materials under stress[2,3]. Here we present an experimental study of crack growth in a two-dimensional system, using a monolayer of uniformly sized microspheres confined between two parallel sheets of glass. The cracking patterns observed in this system closely resemble those found in more complex systems of practical importance, such as paint films or ceramic-coated metals. A simple two-dimensional computer model for elastic fracture leads to structures that closely resemble those observed in the experiments. In both the experimental and computer models an early stage in which isolated defects are formed is followed by a period in which rapid growth of almost linear cracks occurs. At later times the crack growth process slows down and the shapes of the cracks become increasingly irregular.

The two-dimensional material used in our experiments was prepared from uniformly sized spheres of sulphonated polystyrene with an effective diameter d_1 of 3.4 μm (±1%) dispersed in water[4]. By confining the spheres between parallel planar glass sheets it was possible to form a polycrystalline monolayer with a relatively large grain size (typically 10^5–10^6 spheres). A strained film was produced by allowing the monolayer to slowly dry. During this drying process the sphere diameter is reduced to $d_0 = 2.7$ μm.

A variety of different features was observed in the strained film. The first cracks were formed along the grain boundaries and had a tendency to pass through lattice defects such as vacancies and impurities. But here we are concerned primarily with crack propagation inside regular grains with relatively few defects. At the earliest stage in the cracking process, small (localized) defects are formed at a relatively slow rate. This stage is followed by the fast propagation of more-or-less linear cracks (Fig. 1*a*). In the later stages the crack growth process becomes slower and the cracks become progressively less linear (Fig. 2*a*).

Results from a simple two-dimensional model which reproduces these characteristics are shown in Figs 1*b* and 2*b*. This model is based on a model for elastic fracture in thin films[5] in which the close-packed monolayer of microspheres is represented by a triangular network of nodes and bonds that initially form a triangular lattice (Fig. 3). Each node is connected to six nearest neighbours by bonds with an equilibrium bond length of l_0 (equivalent to the microsphere diameter, d_0, in the dried monolayer). We assume that the energy associated with this two-dimensional network is given by a harmonic approximation:

$$E_1 = \tfrac{1}{2}k_1 \sum_i (l_i - l_0)^2 \qquad (1)$$

where l_i is the length of the ith bond and k_1 is the bond force constant.

In addition, each of the nodes is assumed to be bonded to an underlying rigid substrate by a relatively weak bond. The energy associated with this bond is given by

$$E_2 = \tfrac{1}{2}k_2 \sum_j |\mathbf{r}_j - \mathbf{r}'_j|^2 \qquad (2)$$

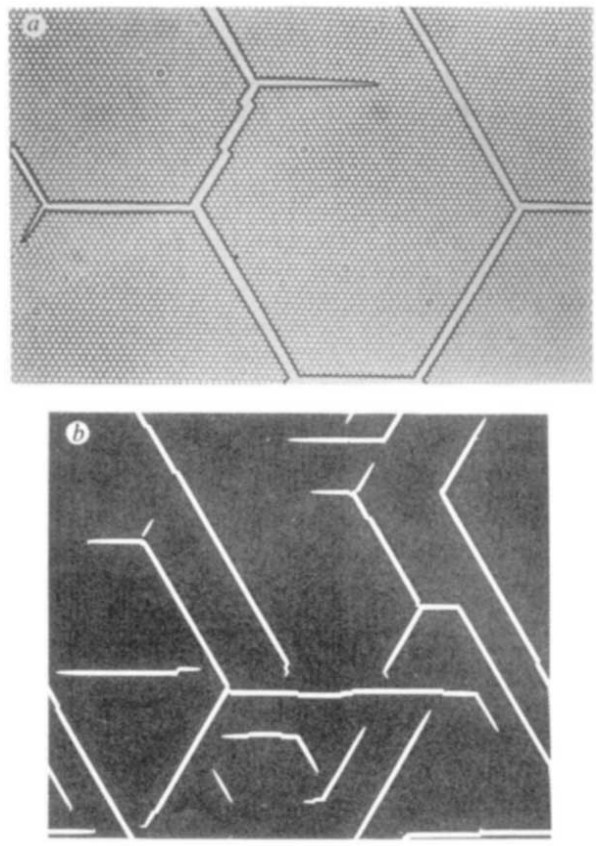

Fig. 1 An early stage in the crack propagation process. *a*, Optical micrograph of a part of a single grain in a much larger system. *b*, Simulation carried out using 40,000 nodes and 120,000 bonds with the parameters $k_1 = 400$, $k_2 = 40$ and $\delta_{max} = 0.25$. The initial strain ($\sigma = l_1/l_0$) was 1.2, which corresponds quite closely to that used in the experiment ($d_1 = 3.4$ μm, $d_0 = 2.7$ μm, $d_1/d_0 = 1.26$); 3,000 bonds have been broken at the stage shown in this figure.

Here $\mathbf{r}_j$ is the position of the jth node and $\mathbf{r}_j$ is the position of attachment to the substrate (denoted by X in Fig. 3).

At the start of each simulation the network is stretched isotropically so that each bond in the triangular network has a length l_1 (equivalent to the diameter d_1 in the experiments). Periodic boundary conditions are used in these simulations so that every node is joined to six nearest neighbours. As the simulation proceeds, bonds in the hexagonal network are selected at random and broken with a probability given by

$$P_i \propto e^{\frac{1}{2}k_1(l_i - l_0)^2} \qquad (3)$$

These probabilities are normalized so that the largest bond-breaking probability associated with any of the bonds is 1.0. After a bond has been broken, the system is relaxed to a new mechanical equilibrium (the energy $E_1 + E_2$ is minimized) and the process is repeated. If, during the mechanical relaxation process, the distance $|\mathbf{r}_j - \mathbf{r}'_j|$ between a node and its point of attachment to the underlying substrate exceeds a value of δ_{max}, then the point of attachment, X, is moved towards the current position of the node until $|\mathbf{r}_j - \mathbf{r}'_j|$ becomes equal to δ_{max}. To avoid 'overshoots' in the movement of the positions of attachment to the substrate, over-relaxation was not used in these simulations. The process of bond-breaking and relaxation is repeated many times to simulate the crack propagation process. These simulations can easily be made time-dependent by incrementing the time by an amount $1/(P_{max}N)$ each time a bond is selected at random (whether or not it is actually broken). Here N is the total number of bonds and P_{max} is the maximum value of $\exp[(k_1/2)\,(l_i - l_0)^2]$ for any bond in the system.

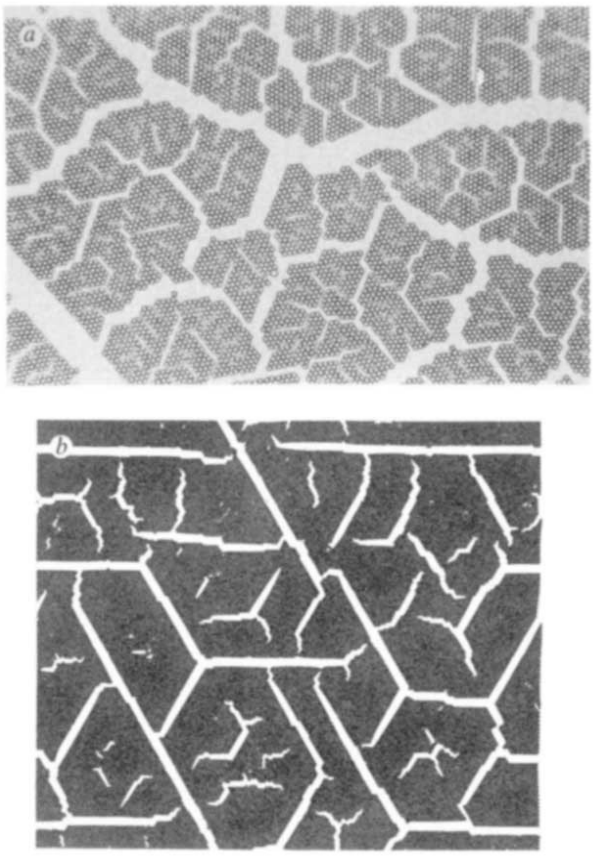

Fig. 2 A relatively late stage in the crack propagation process. *a*, Micrograph obtained from the same experiment as in Fig. 1*a*. *b*, Simulation with $k_1 = 300$, $k_2 = 30$, $\delta_{max} = 0.15$, $\sigma = 1.20$. 7,500 bonds have been broken.

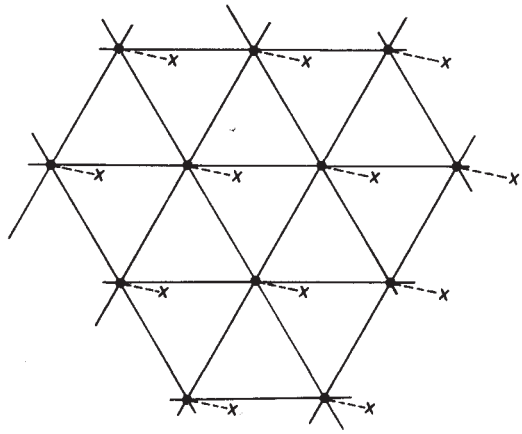

Fig. 3 A representation of the model used in this work. The nodes (large dots) are connected by strong bonds to form a triangular lattice. Each of the nodes is joined to an underlying rigid substrate at X by a weak bond (dashed line). The motion of the nodes is confined to a plane parallel to the substrate. This figure shows the configuration at the start of a simulation.

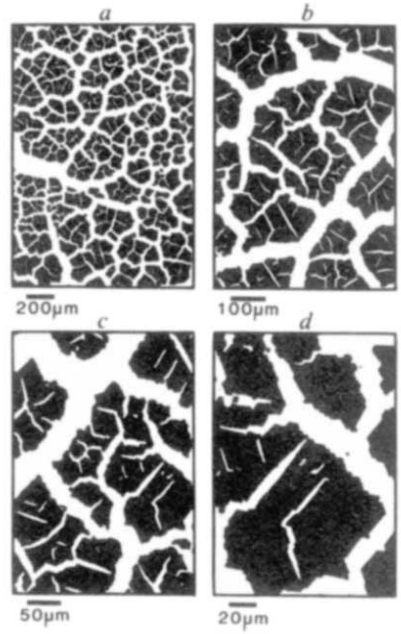

Fig. 4 The final fracture pattern obtained using a monolayer of 3.4-μm spheres. Four different magnifications are shown.

This model is based on the idea that the polymer microspheres are relatively strongly bonded to each other and weakly bonded to the glass surfaces which confine the microspheres to a monolayer. In the model we consider attachment to only one surface but this is equivalent to attachment to both surfaces with bonds which have a force constant of $\frac{1}{2}k_2$. We also assume that the bond-breaking probabilities (crack propagation rates) are very sensitive to the local stress field (as indicated by equation (3)). But the qualitative aspects of our results are not sensitive to the precise form of the relationship between P_i and $(l_i - l_0)$ provided that P_i increases sufficiently rapidly with $(l_i - l_0)$ (ref. 5).

Both the experimental and simulation results are consistent with the following scenario. At the early stages, after the monolayer has dried, the stress is high but the stress concentrations are low. Under these conditions isolated defects are formed relatively slowly. Eventually, some of the isolated defects grow and a large stress concentration builds up at the crack tips. (Alternatively a crack can be induced externally.) Because of the large stress concentration at the ends of the cracks at this stage, they grow very rapidly and the ensuing cracks are almost linear. This initial cracking reduces the average stress in the system, so that subsequent cracking becomes progressively less rapid and the shapes of the cracks increasingly irregular. If there were no bonding between the monolayer and the substrate(s), the stress would be completely relieved after the first few cracks had appeared and no further cracking would occur. Figure 4 shows the fracture pattern at the end of an experiment (at four different magnifications). At the smallest magnification about 500,000 microspheres are shown (compared to the 40,000 nodes used in the simulations), although the experimental system contained a total of $\sim 4 \times 10^7$ spheres.

It has been shown recently that mechanical fracture (cracking) processes in real materials[6,7] may lead to the generation of fractal surfaces. In addition, the results from simple two-dimensional computer models[8,9] also suggest that cracks formed under a variety of conditions may have a fractal geometry. It is now well established that fractal structures are generated by closely related processes such as dielectric breakdown[10] and fluid–fluid displacement processes[11,12], which can be described in terms of the diffusion-limited aggregation (DLA) model[13]. In these processes and in the crack growth model of Louis and Guinea[8], the pattern growth is a non-local process which is controlled by a field which obeys either the Laplace equation[14] (for DLA) or the Navier equation[15] (for crack growth). In our case the weak attachment between the two-dimensional medium and the substrate is sufficient to localize the effects of both isolated and

extended defects[5]. Consequently, the crack-growth process explored here is not closely related to DLA. Nevertheless, the results shown in Fig. 4 do suggest that the cracking patterns might be described in terms of the concepts of fractal geometry[1]. A preliminary investigation (A.T.S., unpublished work), in which the box-counting method[16] was used to analyse digitized representations of Fig. 4 (and similar micrographs), gave an effective fractal dimensionality (D) of 1.68 ± 0.06. That this is quite close to the value found from two-dimensional DLA simulations ($D \simeq 1.71$) (ref. 17) is coincidental.

The cracking patterns generated by these simple experimental and computer models resemble quite closely those found in a variety of more complex systems such as paint films and thin film deposits. We believe that the study of simple model systems can provide valuable insights into the failure of more complex systems which are often of considerable practical importance.

Received 5 July; accepted 2 August 1988.

1. Mandelbrot, B. B. *The Fractal Geometry of Nature* (W. H. Freeman and Company, New York, 1982).
2. *Chemistry and Physics of Fracture* (eds Latanison, R. M. & Jones, R. H.) NATO ASI Series E130 (Martinus Nijhoff, 1987).
3. Atkins, A. G. & Mai, Y. W. *Elastic and Plastic Fracture: Metals, Polymers, Ceramics, Composites, Biological Materials* (Ellis Harwood, Chichester, 1983).
4. Ugelstad, J. *et al. Adv. Colloid & Interface Sci.* **13**, 101-140 (1980).
5. Meakin, P. *Thin Solid Films* **151**, 165-190 (1987).
6. Mandelbrot, B. B., Passoja, D. E. & Paullay, A. J. *Nature* **308**, 721-722 (1984).
7. Avnir, D., Farin, D. & Pfeiffer, P. *Nature* **308**, 261-263 (1984).
8. Louis, E. & Guinea, F. *Europhys. Lett.* **3**, 871-877 (1987).
9. Termonia, Y. & Meakin, P. *Nature* **320**, 429-431 (1986).
10. Niemeyer, L., Pietronero, L. & Wiesmann, H. J. *Phys. Rev. Lett.* **52**, 1033-1036 (1984).
11. Nittmann, J., Daccord, G. & Stanley, H. E. *Nature* **314**, 141-144 (1985)
12. Van Damme, H., Obrecht, F., Levitz, F., Gatinuea, P. & Laroche, C. *Nature* **320**, 731-733 (1986).
13. Witten, T. A. & Sander, L. M. *Phys. Rev. Lett.* **47**, 1400-1403 (1981).
14. Jackson, W. D. *Classical Electrodynamics* (Wiley, New York, 1962).
15. England, A. H. *Complex Variable Methods in Elasticity* (Clowes, London, 1971).
16. Voss, R. F. in *Scaling Phenomena in Disordered Systems* (eds Pynn, R. & Skjeltorp, A. T.) 1-11 (Plenum, New York, 1986).
17. Meakin, P. in *Phase Transitions and Critical Phenomena* Vol. 12 (eds Domb, C. & Lebowitz, J. L.) 336-489 (Academic, New York, 1988).

Seasonal variability of particle flux in the Weddell Sea and its relation to ice cover

Gerhard Fischer*, Dieter Fütterer†, Rainer Gersonde†, Susumu Honjo‡, Dorinda Ostermann‡ & Gerold Wefer*

* Universität Bremen, Geowissenschaften, 2800 Bremen, FRG
† Alfred-Wegener-Institut für Polar- und Meeresforschung, 2850 Bremerhaven, FRG
‡ Woods Hole Oceanographic Institution, Woods Hole, Massachusetts 02543, USA

In the Weddell Sea, primary production varies seasonally as a result of the solar cycle and the large-scale oscillation of the ice edge across much of its area. The annual ice transgression is the largest of any region on Earth[1] and has a profound influence on the production and transportation of particulate matter. In order to clarify the flux, origin and mode of vertical transport of oceanic particles in the pelagic Weddell Sea, we deployed a multi-year sediment trap. The annual particle flux measured was the smallest yet observed in the world ocean, and showed extreme variability. Phytoplankton production is at least partly seeded by diatoms released from the melting of sea ice which had formed in the coastal area of the Antarctic continent. Phytoplankton production under the winter pack ice appears to be minimal.

The year-round mooring station WS-1 is located at 62°26.5′ S, 34°45.5′ W, in a water depth of 3,880 m. This station is covered by sea ice for about 70% of the year (≥9 on ice-cover scale (ICS); see refs 1 and 2). We developed an automated Parflux Mk 5-25 time-series sediment trap[3] at 863 m depth from January 1985 to March 1986; this trap has a 1.2-m^2 opening and is capable of collecting 25 sequential time-specific samples. Based on our results from experiments at the Bransfield Strait[4] we programmed sampling periods of different trapping durations: six periods, each of 11-day duration, were set from 25 January to 1 April 1985; these were followed by 13 periods, of 22-day duration, from 1 April 1985 to 12 January 1986, and finally, another six periods, of 11-day duration, from 12 January to 19 March 1986.

Table 1 Open/close schedule of the sediment trap and particle fluxes

Sample number	Duration (days)	Particle flux ($mg\,m^{-2}\,d^{-1}$)	Days	Calendar date
Open 1	11	0.62	25	25 Jan. 1985
2	11	1.43	36	5 Feb.
3	11	2.92	47	16 Feb.
4	11	3.79	58	27 Feb.
5	11	9.20	69	10 Mar.
6	11	4.66	80	21 Mar.
7	22	0.37	91	1 Apr.
8	22	0.06	113	23 Apr.
9	22	0.02	135	15 May
10	22	0.005	157	6 June
11	22	<0.001	179	28 June
12	22	<0.001	210	20 July
13	22	<0.001	223	11 Aug.
14	22	<0.001	245	2 Sept.
15	22	<0.001	267	24 Sept.
16	22	<0.001	289	16 Oct.
17	22	<0.001	311	7 Nov.
18	22	<0.001	333	29 Nov.
19	22	<0.001	355	21 Dec.
20	11	0.02	377	12 Jan. 1986
21	11	0.11	388	23 Jan.
22	11	0.33	399	3 Feb.
23	11	1.06	410	14 Feb.
24	11	0.30	421	25 Feb.
25	11	0.34	432	8 Mar.
Close			443	19 Mar.

The trap was deployed at the northern Weddell Sea station, 62°26.5′ S, 34°45.5′ W, 863-m water depth. Opening/closing of the trap as controlled by a microprocessor-based timer and the operation was verified by an independent computer after recovery. All opening/closing times were 12:00 noon GMT.

The dry mass flux was collected on preweighed, gridded Nuclepore filters. The amounts of biogenic silica (opal), carbonate and lithogenic particles (clay) were estimated from the Si, Al and Ti content, which were determined by inductively coupled plasma spectrometry analysis (ICPS)[5]. Content of combustible organic matter was estimated as the difference between the total flux and the sum of the opal, carbonate and lithogenic components. These values agreed with results from organic elemental analysis[6].

The annual particle flux measured at the northern Weddell Sea station from 25 January 1985 to 23 January 1986 was 371 $mg\,m^{-2}$, with biogenic opal, combustible matter, carbonate and the clay particles making up 79, 17, 3 and 1% of the total flux, respectively. Biogenic material comprised 99% of the total flux. The seasonal variability in the daily flux was very high (Fig. 1), ranging from a maximum flux of 9.2 $mg\,m^{-2}$ per day during March 1985 to almost zero for July 1985 to January 1986.

Significant particle flux occurred from the start of the experiment, when sea ice retreated southwards of the mooring site. The flux increased rapidly and reached its maximum about 10 weeks after the ice opened, at which time the ice edge had retreated about 950 km to the south of the station (Fig. 1). Ice around the mooring site loosened at the beginning of 1986, and the ice edge passed the station at the end of January 1986. During the 1986 study period, the flux maximum occurred between February 14 and 25 (sample 23), about six weeks earlier